Flow Measurement and Instrumentation 50 (2016) 229–236

Contents lists available at ScienceDirect

Flow Measurement and Instrumentation

journal homepage: www.elsevier.com/locate/flowmeasinst

Natural gas compositions variation effect on capillary tube thermal mass flow meter performance

S. Parvizi [a], A. Arabkoohsar [b,*], M. Farzaneh-Gord [a]

[a] Faculty of Mechanical Engineering, Shahrood University of Technology, Shahrood, Iran
[b] Department of Mechanical Engineering, Azadshahr Branch, Islamic Azad University, Azadshahr, Iran

ARTICLE INFO

Article history:
Received 28 May 2016
Received in revised form
10 July 2016
Accepted 21 July 2016
Available online 22 July 2016

Keywords:
Capillary tube thermal flow meter
Natural gas
Compositions variation
Error analysis

ABSTRACT

Thermal mass flow meters are broadly used in different parts of industry for flow metering objectives from very low up to very high flow rates. One of the most widely used thermal flow meters is capillary tube type which is more appropriate for measuring low mass flow rates. On the other hand, natural gas measurement accuracy in residential use has already been studied by the authors and it was found out that considerable amount of natural gas is lost over the year due to inaccurate flow metering. In order to resolve this problem, employing capillary tube mass flow meters instead of conventional counters in houses, assuming natural gas as pure methane, was proposed and investigated, resulting to satisfactory outcomes. Although pure methane well estimates natural gas behavior in many cases, it may not be an accurate assumption for heavy natural gas mixtures composed of lower methane fractions. Therefore, in this work, the effect of natural gas compositions variation on the performance of capillary tube thermal mass flow meters in residential use is studied. For this objective, various natural gas fields of Iran are considered and differential equations of natural gas stream and sensor tube are solved contemporary in Matlab. In the end, in order to validate the simulation approach and conditions, the simulation was accomplished for Nitrogen, for which experimental data was available in the literature. The results show that using an average specific heat capacity value for different mixtures causes a deviation below a maximum of only 1.8% and overall average error of 0.62% in measurement accuracy. It was also found out that changes in other properties of natural gas does not affect the accuracy.

1. Introduction

In natural gas industry, in many cases, mass flow metering is preferred to volume flow metering. Measuring volume flow rate of natural gas is not difficult nowadays as several accurate devices such as multiple ultrasonic transient-time meters, conventional orifice plates and turbine meters are available and could be used for this objective [1]. On the other hand, natural gas mass flow rate also could be measured by employing some instruments such as coriolis density meters, mass flow controllers and gas chromatographs, which basically calculate natural gas density, along with the aforementioned volume flow meters. However, one should note that some technical drawbacks such as costly operation and disability in drift detection restricted these instruments to be broadly employed for natural gas mass flow metering [2]. In addition to employing these devices for mass flow metering, two more different measures are also possible to be taken. The first approach is measuring volume flow rate and then multiplying this value by the natural gas density which is calculable by natural gas EOSs (equation of states) such as AGA8 for which the mixture compositions along with its temperature and pressure values should be known [3,4]. The other measure is employing thermal flow meters which are less affected by temperature and pressure changes. A thermal mass flow meter imposes heat to the fluid stream and measures the amount of dissipated heat, which is a functional of the given fluid thermal properties. Therefore, thermal flow meters are more suitable for the applications in which thermal properties of fluid remain constant during actual operation. It is also noteworthy that thermal flow meters are only appropriate for gas flows because of heat absorption problem in liquid flows [5].

Natural gas mass flow rate consumed by an individual consumer in residential users' category is usually in very low range of 0–4 m^3/h (flow rates up to 6 m^3/h may also seldom be observed). In Iran, and many other countries of the world, diaphragm volume flow meters are used to meter natural gas consumption of this sector [6]. The inability of accurate metering in low flow rates

* Corresponding author.
E-mail address: mani.koohsar@yahoo.com (A. Arabkoohsar).

http://dx.doi.org/10.1016/j.flowmeasinst.2016.07.007
0955-5986/

Nomenclature

A	Heat transfer area m^2
c_p	Constant pressure specific heat capacity kJ/(kg K)
D_{in}	Internal diameter of sensor tube m
D_{out}	External diameter of sensor tube m
h_i	Internal convective heat transfer coefficient W/(m^2 K)
k	Thermal conductivity coefficient kJ/(m K)
l	Length m
L_s	Sensor position on the sensor tube m
$\dot{m}_1$	Inlet mass flow rate kg/s
$\dot{m}_2$	Outlet mass flow rate kg/s
N	Number of tubes in laminar flow element
p	Wetted perimeter m
P	Pressure kPa
ΔP_s	Pressure drop in sensor tube kPa
ΔP_{LFE}	Pressure drop in laminar tube element kPa
q	Heat transfer/flux kJ or kW
R	Thermal resistance per unit length for radial heat loss (m K)/W
S	Sensitivity of flow meter (K s)/kg
ΔT	Temperature difference between the sensors °C or K
T	Temperature °C or K
T_a	Ambient Temperature °C or K
V_z	Velocity component in direction of length m/s
V_r	Velocity component in direction of radius m/s
V_θ	Velocity component in direction of angle m/s

Greek symbols

μ	Viscosity Pa s
ρ	Density kg/m^3
υ	Kinematic viscosity m^2/s

(below 1 m^3/h) causes this instrument to not be completely reliable and this is why considerable volume of natural gas loss occurs in residential natural gas distribution network [7]. According to National Iranian Gas Company (NIGC), there was over 9 BCM (billion cube meter) difference between the measured values in the supplied and the consumed parts of residential section in 2013 [8].

Therefore, Farzaneh-Gord et al. [9] proposed employing capillary tube thermal mass flow meters, which are very suitable for low mass flow rate ranges, to be used instead of conventional counters of natural gas flow rate in residential section. In that work, they considered natural gas as pure methane to investigate the feasibility of using such mass flow meters and obtained satisfactory results with an overall error of below 1.5%. Clearly, changing the fraction of methane in natural gas composition may affect the measurement accuracy. Thus, in this work, the effect of natural gas compositions variation on the proficiency of a capillary tube thermal flow meter designed for residential use natural gas measurement is investigated. For this objective, the performance of the capillary tube flow meter proposed in Ref. [9] is assessed for 6 natural gas fields of Iran, including very light to very heavy (sour) mixtures. In this way, not only the effect of changing methane fraction in natural gas compositions on the accuracy of the device is investigated, but also its performance is assessed for real natural gas fields in the widest possible methane fraction range.

2. Capillary tube thermal mass flow meters

Thermal mass flow meters employ heat to measure the flow rate by imposing a specific amount of heat to the fluid stream and measuring the amount of dissipated heat [10]. In terms of measuring the amount of dissipated heat, these devices are divided into two categories, namely, constant temperature differential and constant current. Both of these methods employ two temperature sensors, one as the heated part sensor and another one measuring the stream temperature [11]. In contrast with the constant temperature differential approach in which mass flow rate is measured based on the value of electrical power required to keep the two sensors temperature difference constant, the power value is constant and mass flow rate is directly a functional of the sensors temperature difference in constant current method [12–14]. Also, in terms of operation principles, thermal mass flow meters are classified into two categories as immersible and capillary tube mass flow meters, which are respectively appropriate for high and low mass flow rates [15,16]. This is why capillary tube thermal flow meters are proposed to be used in this work. Fig. 1 illustrates the schematic diagram of capillary tube thermal mass flow meters.

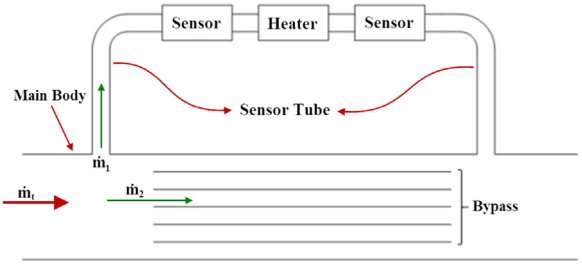

Fig. 1. The schematic diagram of a capillary tube thermal mass flow meter.

As the figure shows, the inlet stream flows through two different paths, i.e. the sensor tube with minor portion of the total mass flow rate ($\dot{m}_1$) and the laminar flow element (the bypass line) with major portion of the total flow ($\dot{m}_2$). The laminar flow element consists of N tubes with the same characteristics as the sensor tube and keeps the stream in laminar regime so that the proportion of $\dot{m}_1$–$\dot{m}_2$ remains fixed and the pressure reduction along this element causes the flow portion through the sensor tube to be trifle [17]. According to Fig. 1, for mass flow rate through a capillary tube thermal mass flow meter, one has:

$$\dot{m}_t = \dot{m}_1 + \dot{m}_2 = \dot{m}_1\left(1 + \frac{\dot{m}_2}{\dot{m}_1}\right) = \beta\,\dot{m}_1 \tag{1}$$

The value of β in this equation is called bypass proportion and depends on the amount of pressure reduction through the laminar flow element (ΔP_{BP}). Considering the flow through the bypass as a laminar and fully developed flow, one has [18]:

$$\Delta P_{BP} = \frac{128\cdot\mu\cdot l}{\rho\cdot N\cdot\pi\cdot D_{in}^{\ 4}}\ \dot{m}_2 \tag{2}$$

where D_{in}, l, ρ and μ are respectively the internal diameter and length of each tube in laminar flow element, the fluid density and its dynamic viscosity. Also, by the same token and taking the same assumptions as the flow within the laminar flow element tubes, one could calculate the amount of pressure drop through the sensor tube (ΔP_s) as below:

$$\Delta P_s = \frac{128\cdot\mu\cdot l}{\rho\cdot\pi\cdot D_{in}^{\ 4}}\ \dot{m}_1 \tag{3}$$

Evidently, the pressure values at the initial and final points of

Please cite this article as: S. Parvizi, et al., Natural gas compositions variation effect on capillary tube thermal mass flow meter performance, Flow Measurement and Instrumentation (2016), http://dx.doi.org/10.1016/j.flowmeasinst.2016.07.007

the sensor tube and laminar flow element are equal, thus:

$$\begin{cases} \Delta P_{BP} = \Delta P_s \quad \Rightarrow \quad \dfrac{\dot{m}_2}{\dot{m}_1} = N \\ \qquad\qquad \Rightarrow \dot{m}_t = (1+N)\ \dot{m}_1 \quad \Rightarrow \beta = N+1 \\ \dot{m}_t = \left(1+\dfrac{\dot{m}_2}{\dot{m}_1}\right)\dot{m}_1 = \beta\,\dot{m}_1 \end{cases} \tag{4}$$

This equation applies for any kind of bypass line regardless the geometry, in case of having a laminar and fully developed flow. In fact, this equation is the primary principle operation of thermal mass flow meters and demonstrates that the bypass proportion is always a constant value and independent of any gas flow physical properties. Therefore, measuring the mass flow rate passing through the sensor tube and having the value of bypass proportion, one could easily calculate the total mass flow rate. This is why measuring the mass flow rate through the sensor tube is only discussed here.

According to Fig. 1, there are three elements, namely, two sensors and a heater on the sensor tube of a capillary tube flow meter. The heater is located in the middle of the sensor tube and the sensors are located with the same distance from the heater on its right and left hands. In fact, the operation principle is so that the sensor tube is first heated and this heat is absorbed by the fluid stream while passing through the sensor tube in upstream. In other words, in upstream the heat is transferred from the warmed sensor tube to the fluid and in downstream the heated fluid gives this heat back to the sensor tube and as a result, a temperature difference (ΔT) by the sensors is measured. The value of ΔT depends on the fluid mass flow rate so that increasing the flow rate picks the ΔT value up to higher levels. Therefore, when mass flow rate is zero, both of the sensors report similar temperature values and ΔT is zero [17]. On the other hand, for this type of flow meter, as long as ΔT is a linear functional of mass flow rate changes, the metering task is done accurately; otherwise, the measurement accuracy could be affected. In other words, the device performance is only reliable for a mass flow rate range in which ΔT value changes linearly.

Fig. 2 shows these operation principles schematically for a typical capillary tube flow meter with sample characteristics. This figure, actually, includes two sections: part (a) illustrates the temperature distribution profile of fluid stream along the length of the sensor tube (z axis) for two sample flow rates i.e. 0 and 50 standard cubic centimeters per minute (sccm, where standard condition is considered as P=100 kPa and T=25 °C) and part (b) shows how one could specify the accurate metering range of a capillary tube thermal flow meter by defining the linearity range of ΔT value change versus flow rate variations. In Fig. 2a, as can be seen, the temperature distribution profile associated with flow rate zero is symmetric (the green graph) and this means that ΔT=0 in this case. As it was explained, the range of linearity in Fig. 2b is an important parameter as it determines the reliable range of flow metering for the device. The slope angle of linear section in this figure also determines the sensitivity of the device relative to mass flow rate variations, given by [9]:

$$S = \frac{\partial\left(T_s|_{z=+20} - T_s|_{z=-20}\right)}{\partial\,\dot{m}} \tag{5}$$

The higher values of sensitivity for a device make it a more accurate and reliable measurement instrument. It is noteworthy that these figures have been provided based on volume flow rates as presenting general information about capillary tube flow meters is only intended in this section and the same figures based on mass flow rate could easily be presented.

3. Simulation and validation procedures

In this section, the numerical simulation carried out on the device for simulating the natural gas flow through the sensor tube of a capillary tube flow meter and the validation process for proving the accuracy of the obtained results are presented.

3.1. Numerical simulation

As it was explained, the main operation principle of thermal mass flow meters is based on heat transfer between the capillary sensor tube and the gas flow. For solving the heat transfer equations, energy balance equations for both of the sensor tube and the fluid stream should be written separately. The general format of energy equation for a stream in steady state in cylindrical coordinate system is [19]:

$$V_r\left(\frac{\partial T}{\partial r}\right) + \frac{V_\theta}{r}\left(\frac{\partial T}{\partial \theta}\right) + V_z\left(\frac{\partial T}{\partial z}\right) = \frac{k}{\rho\ c_p}\left(\frac{1}{r}\frac{\partial}{\partial r}\left(r\frac{\partial T}{\partial r}\right) + \frac{1}{r^2}\frac{\partial^2 T}{\partial \theta^2} + \frac{\partial^2 T}{\partial z^2}\right) + \frac{q}{\rho \cdot c_p} \tag{6}$$

where V_r, V_θ and V_z are the fluid velocity components in the three different cylindrical directions. Also, T, k, ρ and c_p refer to the temperature, thermal conductivity coefficient, density and constant pressure specific heat capacity of fluid, respectively. Also, q

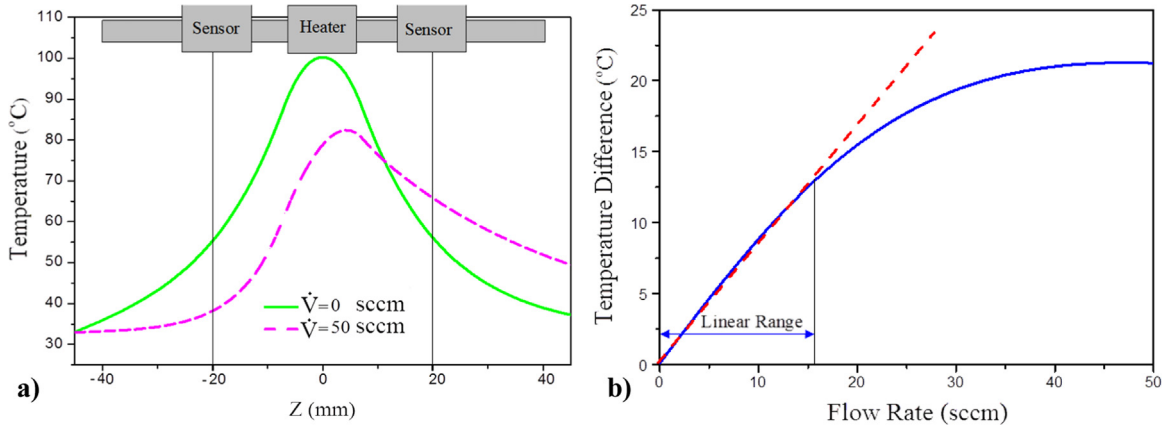

Fig. 2. The schematic diagram of a capillary tube flow meter operation principle; a) temperature distribution graph along the sensor tube, b) indicating accurate measurement range for the device by temperature difference variation versus flow rate changes.

Please cite this article as: S. Parvizi, et al., Natural gas compositions variation effect on capillary tube thermal mass flow meter performance, Flow Measurement and Instrumentation (2016), http://dx.doi.org/10.1016/j.flowmeasinst.2016.07.007

Table 1
The thermal and technical information about the thermal mass flow meter.

Diameter of the inlet sectional area	50 mm
Length of heater on the sensor tube	14.8 mm
Heat flux intensity	500 W/m^2
Sensor tube internal diameter	0.977 mm
Sensor tube external diameter	1.257 mm
Sensor tube length	90 mm
Sensors positions	$\pm$7.5 mm
Insulator material	Mineral wool
Insulator thermal conductivity	0.0927 W/(m K)
Insulator specific heat capacity	0.84 kJ/(kg K)
Insulator density	50 kg/m^3
Insulator thickness	19.275 mm

represents the amount of heat transfer from/to the fluid. Taking this equation into account, for the fluid stream within the sensor tube, by neglecting heat transfer and temperature gradient in directions of θ and r, one could write:

$$k_f A_f \frac{d^2T_f}{dz^2} - \dot{m} c_f \frac{dT_f}{dz} + h_i p_t (T_t - T_f) = 0 \quad (7)$$

In which, the first, the second and the third items of the equation refer to the axial heat conduction, enthalpy variation in the fluid and convective heat transfer from the fluid to the sensor tube body, respectively. Also, for the sensor tube, one has:

$$k_t A_t \frac{d^2T_t}{dz^2} + h_i p_t (T_f - T_t) - \frac{1}{R}(T_t - T_a) + q' = 0 \quad (8)$$

In which, the first to the third parameters on the left side of the equation are respectively the axial conductive heat transfer, convective heat transfer rate between the fluid and tube and radial heat loss from the tube to the environment. Note that, in these two equations, the parameters A, h_i, p and R refer to the cross sectional area, the convective heat transfer coefficient between the fluid and tube, the wetted perimeter and thermal resistance per unit length for radial heat loss, respectively. The subscriptions f, t and a also represent the fluid, the sensor tube and environment. The following boundary conditions are taken into account for solving this problem:

$$\begin{cases} T_t|_{z=-L} = T_f|_{z=-L} = T_a \\ T_t|_{z\to\infty} = T_f|_{z\to\infty} = 0 \end{cases} \quad (9)$$

Note that L is equal to half of the total length of sensor tube. It is also noteworthy that for solving this problem numerically, finite volume methods have been used to discrete the equations and the solution has been carried out by SHOOTING method in MATLAB programming language. Besides, some assumptions as state conditions for simulating the system have been made; e.g. some parameters have been considered to be constant i.e. the velocity of the fluid through the sensor tube, the heat flux supplied by the heater, the convection rate inside the tube and convection rate from the heater insulator to the environment.

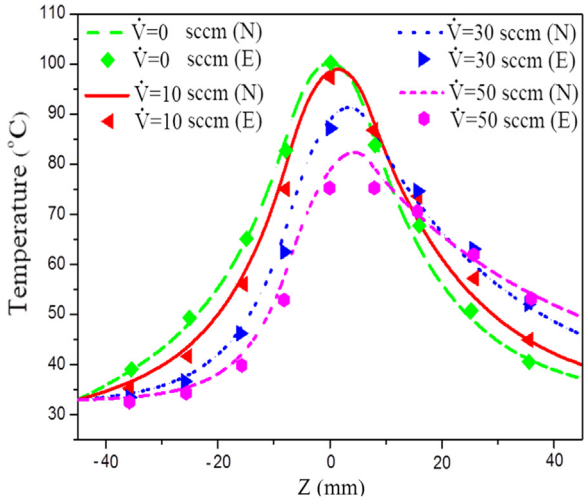

Fig. 4. Comparison of temperature distribution along the sensor tube in the experimental and numerical simulation.

Table 1 presents information about all of the characteristics considered for the device during the numerical simulation and the details of selecting these characteristics will be discussed in results section.

3.2. Validation of numerical solution

In this section, the numerical method taken for simulating natural gas stream through a sensor tube is going to be validated. Naturally, there should be an experimental set to compare the results of numerical and experimental investigations for this objective. It is noteworthy that no experimental facilities were employed for this work as there is an experimental study carried out for nitrogen available in literature [20]. At first sight, this question may arise that whether or not it is reasonable to validate numerical results for a natural gas mixture, which is mainly formed by methane (over 80%), by employing experimental results associated with nitrogen. To justify this issue, one should note that natural gas consumed in residential section behaves extremely like an ideal gas as its pressure is only 1.7 kPag. On the other hand, nitrogen state also is very similar to an ideal gas in this pressure range. As a result, the results could be compared and the numerical simulation approach taken could be confirmed in case of obtaining the same results. For this objective, the numerical solution is first done for nitrogen in the same conditions as reported in Ref. [20] and if the numerical simulation results match the experimental results, the solution can also be done for natural gas. Fig. 3 illustrates the experimental setup employed in this work in which

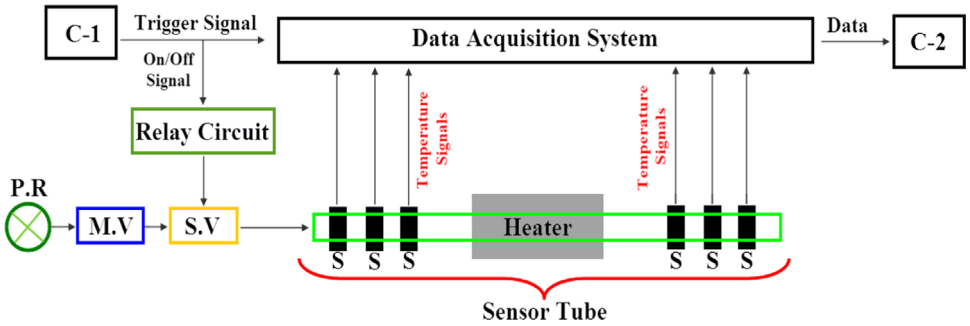

Fig. 3. Experimental setup in Ref. [20]; C: computer, P.R: pressure regulator, M.V: metering valve, S.V: soleniod valve, S: temperature sensor.

Please cite this article as: S. Parvizi, et al., Natural gas compositions variation effect on capillary tube thermal mass flow meter performance, Flow Measurement and Instrumentation (2016), http://dx.doi.org/10.1016/j.flowmeasinst.2016.07.007

the length of sensor tube, internal and external diameters of sensor tube and length of heater are 91 mm, 0.977 mm, 1.257 mm and 14.8 mm, respectively. In this experiment, the sensor tube material is stainless steel 304; the heating wire is made of 80% nickel and 20% chromium. The experiment was done for various flow rates from 0 to 50 sccm with an uncertainty in range of $\pm 1\%$.

Fig. 4 shows the results of numerical simulation carried out on such a sensor tube for nitrogen and the same boundary conditions and circumstances as those considered by Kim et al. [20] and makes a comparison between the obtained values from the numerical simulation and the values given in the experimental study. In this figure *N* and *E* refer to the results associated with the numerical and experimental studies, respectively.

According to the figure, the experimental study just provided temperature distribution graphs for four flow rates (0, 10, 30 and 50 sccm) and, inevitably, the simulation results could only be given for these four volume flow rates to show the possible deviation or accuracy in different flow rate values. Evidently, the results of numerical simulation are highly close to the measured values in the experimental study for all of the four considered flow rates along the sensor tube. It should be noted that although the temperature distribution profiles are important, in mass flow metering, the difference between the values measured by the two main sensors which have been located in $L_s = \pm 7.5$ mm are the most important parameters. Obviously from the figure, even for this range of *Z*, the deviations of numerical results from the experimental results are still negligible.

Also, as an assumption taken during the simulation, gas density has been considered to be constant and it should be justified if it is a reasonable assumption or not. For the sake of clarification, it can be said that temperature variation range along the entire length of the sensor tube is always below 60 °C and clearly, considering an average density may not affect the measurement accuracy as the maximum deviation of the average density from the actual density value in this temperature change range is less than 7%. In addition, not only the value of average density is only required for resolving the energy conservation equation (and subsequently plotting the temperature distribution profiles) and it does not contribute in mass flow metering process directly, but also the important section in the temperature profile is the section between the main sensors where temperature difference is in range of 0–10 °C in which density deviation is only about 1%. Therefore, one could claim that this assumption is totally reasonable due to its negligible effect on the calculation process and it does not affect the metering accuracy.

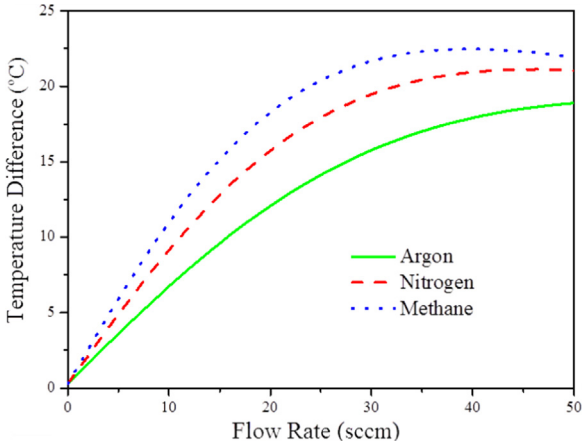

Fig. 5. Comparing the sensitivity and linearity range of flow metering for different gases based on flow rate changes.

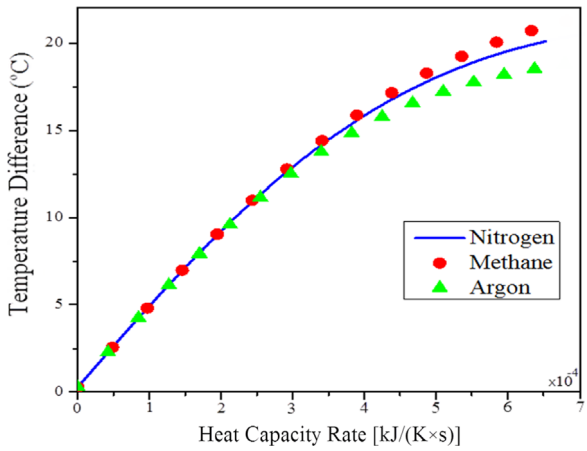

Fig. 6. Comparing the sensitivity and linearity range of the device for different gases based on heat capacity rate changes.

Table 2
The percentage of compositions of different natural gas fields of Iran and their specific heat and density values in standard condition (100 kPa and 25 °C).

	Torkman	Kangan	Khangiran	Gonbadly	Pars	Bidboland
CH4	94.21	90.04	98.6	88.05	87	80.01
C2H6	2.25	3.69	0.59	1.4	5.4	1.38
C3H8	0.53	0.93	0.09	0.34	1.7	0.49
I-C4H10	0.36	0.2	0.02	0.09	0.3	0.34
N-C4H10	0	0.29	0.04	0.13	0.45	0.65
I-C5H12	0.26	0.14	0.02	0.07	0.13	0.10
N-C5H12	0	0.08	0.02	0.06	0.11	0.09
N-C6H14	0.17	0.14	0.07	0.03	0.07	0.09
+C7H16	0.18	0.01	0	0.33	0.03	0
N2	1.9	4.48	0.55	7.85	3.1	5.41
CO2	0.14	0	0	1.63	1.71	8.41
H2S	0	0	0	0	0	3.03
H20	0	0	0	0.02	0	0
MW [kg/kmol]	17.34	17.79	16.36	18.17	18.69	20.51
c_p[kJ/(kg K)]	2.139	2.086	2.208	1.998	2.031	2.071
***P* [kg/m^3]**	0.701	0.719	0.659	0.735	0.756	0.772

4. Results and discussions

After confirming the accuracy and validation of the taken numerical simulation for nitrogen, the simulation is going to be accomplished for a capillary tube flow meter with the characteristics detailed in Table 1 for 6 major natural gas fields of Iran. In this section, the results of these investigations are presented.

In this regards, first of all, the sensitivity of the device is assessed for different gases to evaluate if a specific thermal flow meter could be used for measuring the mass flow rate of every gas. Fig. 5 shows the variation of temperature difference (ΔT) versus flow rate variations for three different gases, namely, nitrogen, methane and argon.

According to the figure, the curve inclination in the linear range and the linearity range for the gases are totally different and this means that flow rate is not an appropriate index for different gases while using the same thermal flow meter.

For solving this problem, the novel index of heat capacity rate (i.e. mass flow rate multiplied by the specific heat capacity of each of these gases) is defined and proposed to be used in this work. Therefore, Fig. 6 illustrates ΔT value variation based on heat capacity rate changes of these gases. Obviously, the linearity range and sensitivity of the capillary tube thermal flow meter for different gases are the same and this means that having the specific heat capacity of each gas, this device could be used for measuring

Please cite this article as: S. Parvizi, et al., Natural gas compositions variation effect on capillary tube thermal mass flow meter performance, Flow Measurement and Instrumentation (2016), http://dx.doi.org/10.1016/j.flowmeasinst.2016.07.007

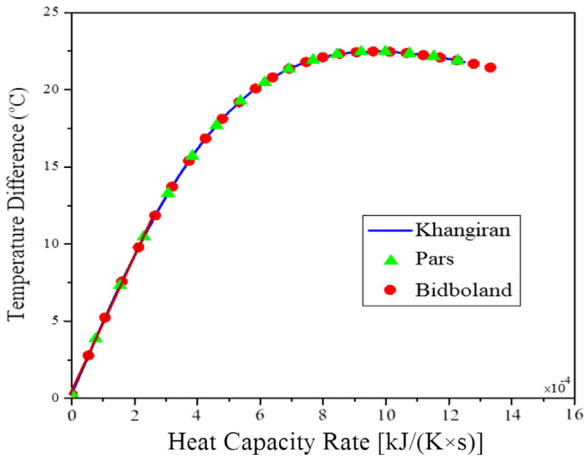

Fig. 7. Linearity range determination and comparison for three different natural gas mixtures.

Table 3
The effect of natural gas pressure changes on its density and heat capacity values in a constant temperature.

	1 kPa		50 kPa		100 kPa	
	c_p [kJ/(kg K)]	ρ [kg/m^3]	c_p [kJ/(kg K)]	ρ [kg/m^3]	c_p [kJ/(kg K)]	ρ [kg/m^3]
Torkman	2.139	0.708	2.142	1.052	2.145	1.405
Kangan	2.086	0.726	2.089	1.080	2.092	1.441
Khangiran	2.220	0.675	2.223	1.003	2.226	1.339
Gonbadly	2.001	0.743	2.004	1.104	2.006	1.473
Pars	2.029	0.762	2.032	1.132	2.036	1.511
Bidboland	1.802	0.841	1.805	1.251	1.808	1.669

the mass flow rate of different gases, resulting to accurate measurement.

Hereafter, the 6 actual gas mixtures which are the main natural gas fields of Iran are considered to evaluate the effect of natural gas compositions changes on the sensitivity alteration and linearity range variation and to verify whether or not the device could be used for metering different natural gas mixtures mass flow rates. Table 2 details the compositions of these natural gases provided by NIGC, Semnan division.

According to the table, in all cases, natural gas mainly comprises of methane (at least 80%) and some heavy hydrocarbons like ethane, propane and butane with minor proportions. There may be also some other substances like carbon-dioxide, nitrogen and

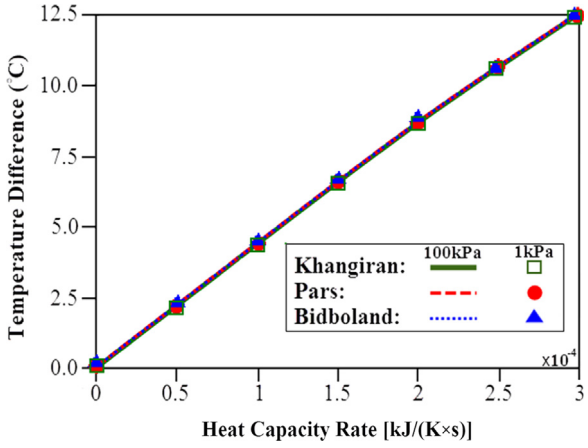

Fig. 8. Pressure variation effect on the performance of the device for metering three different mixtures.

Table 4
The effect of natural gas temperature change in a constant pressure on its density and heat capacity values.

	0 °C		15 °C		30 °C	
	c_p [kJ/(kg K)]	ρ [kg/m^3]	c_p [kJ/(kg K)]	ρ [kg/m^3]	c_p [kJ/(kg K)]	ρ [kg/m^3]
Torkman	2.086	0.958	2.118	0.907	2.153	0.862
Kangan	2.035	0.983	2.065	0.931	2.101	0.885
Khangiran	2.155	0.901	2.184	0.853	2.217	0.811
Gonbadly	1.949	1.001	1.977	0.948	2.007	0.901
Pars	1.968	1.024	1.999	0.971	2.035	0.922
Bidboland	1.759	1.138	1.785	1.078	1.814	1.024

hydrogen sulfide in the compositions for which the proportions could vary significantly from a specific natural gas field to another one. Overall, a natural gas mixture with higher proportion of methane is a lighter mixture (like Khangiran) while a natural gas with lower proportion of methane is a heavier mixture. For the mixtures with low methane share (as low as 80%) and high heavy hydrocarbons portions (like Bidboland), the composition is called sour gas.

Therefore, the first step is to evaluate the performance of such a capillary tube flow meter for three different natural gases in the widest range of molecular weights (from very light to very heavy mixtures) in terms of the variation of ΔT against heat capacity changes. In this way, not only the accuracy of the device could be verified, but also the linearity range for different ranges of molecular weights could be found and compared. Fig. 7 illustrates this issue for the lightest mixture among all the considered fields (Khangiran), the mixture with middle range of heaviness (Pars) and the heaviest mixture which is a sour gas (Bidboland).

According to the figure, ΔT varies linearly for the three cases up to an almost the same value of heat capacity i.e. well above 3×10^{-4} kJ/(K s). Also, it is obvious that the obtained values for ΔT from the numerical simulations in all ranges of heat capacity (even up to the highest considered heat capacity value) are very close to each other.

As two important factors, the effect of natural gas stream pressure and temperature variations on the curve of different gases in ΔT-heat capacity rate coordinate and subsequently, the measurement accuracy should be investigated. Firstly, Table 3 shows the values of density and specific heat capacity of different mixtures for three different pressures (very low: 1 kPa, middle range: 50 kPa and very high: 100 kPa) in a specific temperature (T=25 °C). Note that gauge pressure is considered here as the standard pressure in residential distribution pipelines is 1.7 kPag.

Subsequently, Fig. 8 shows if this trifle change occurred in density and specific heat capacity due to pressure change could affect the value of ΔT versus heat capacity rate variations. This figure has also been provided for the three lightest (Khangiran), heaviest (Bidboland) and semi-heavy (Pars) fields, for the lowest and highest pressures considered in Table 3.

According to the figure, the effect of pressure change, even in the conservative considered range, on the density and specific heat capacity of these gases is so slight that it does not affect the thermal flow meter performance for any of these gases considerably.

Similarly, in the next step, the effect of temperature change is assessed. The investigations show that in Tehran, as the case study of this work, ambient temperature varies from well above 0 °C in winter up to 30 °C in summer and temperatures out of this range are rarely monitored. Therefore, Table 4 considers three temperatures of 0 °C, 15 °C and 30 °C to cover all the possible temperatures in this city to investigate the effect of temperature

Please cite this article as: S. Parvizi, et al., Natural gas compositions variation effect on capillary tube thermal mass flow meter performance, Flow Measurement and Instrumentation (2016), http://dx.doi.org/10.1016/j.flowmeasinst.2016.07.007

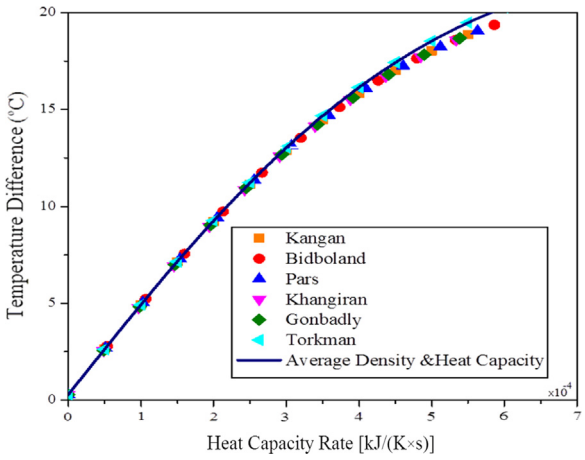

Fig. 9. Deviation of measurement values for different natural gas fields relative to the selected reference measurement curve.

change on natural gas density and specific heat values in a constant sample pressure of 125 kPa.

In this case also, the same results as pressure change effects are obtained and, in other words, no significant change on the performance of the thermal flow meter for any of these gases was observed. As the plotted figure in this assessment was extremely similar to Fig. 8, in order to avoid presenting a repetitive graph, no figure is presented for this assessment.

According to the above figures and graphs, a very good accuracy measurement for all of the considered natural gas compositions could be expected if a specific reference operation curve is defined properly for the device. Actually, the reference operation curve is a curve in ΔT-heat capacity rate coordinate system which estimates the minimum overall deviation relative to the actual ΔT value of different gases. For this objective, the curve related to a mixture with the averaged values of density and specific heat capacity of all of these six gases in standard conditions is proposed to be considered as the reference operation curve of the device. By this method, in case of obtaining satisfactory results, not only the operation reference curve of the capillary tube thermal flow meter for natural gas metering is found, but also the z-axis, which is currently based on the non-readable parameter of heat capacity rate, could be easily converted to mass flow rate ($\dot{m}$=heat capacity rate divided by specific heat capacity).

Fig. 9 shows the simulation results for different natural gas mixtures versus the reference operation curve associated with the averaged values of specific heat capacity [2.088 kJ/(kg K)] and density [0.723 kg/m^3]. Obviously from the figure, the values related to all of the 6 gases almost lie on the reference curve in the linear range, though thereafter the accuracy decreases considerably. Clearly, taking the average specific heat value into account, the linearity range 0 to 3×10^{-4} kJ/(kg K) is converted to 0–0.517 kg/h. It should be noted that this mass flow metering range is for the sensor tube only. Therefore, for being able to cover the entire possible natural gas mass flow rate range in residential use (from 0 up to a maximum of almost 4.5 kg/h), according to Eq. 4, the capillary tube thermal flow meter should have 8 tubes the same as the sensor tube characterized in Table 1 in bypass route (β=9).

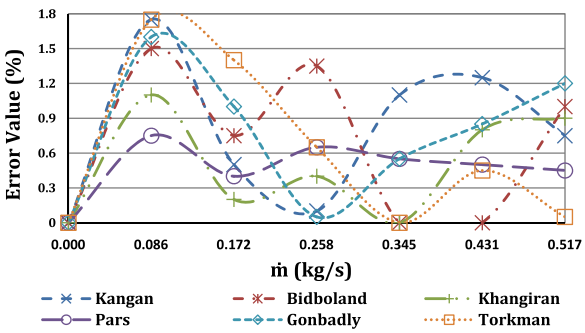

Fig. 10. Error values for different natural gas mixtures in the linear range.

Finally, considering the explanation presented and the above figure, taking into account the value of averaged specific heat and calculating the slope angle of the reference operation curve in its linear section; one could calculate the natural gas mass flow rate as a linear functional of ΔT value measured by the capillary tube sensors as follow:

$$\dot{m}_t = (8+1)\dot{m}_1; \qquad \text{Where:}\dot{m}_1 = 11\times10^{-5}\times\Delta T \tag{10}$$

In this regards, Fig. 10 shows the values of errors observed for different natural gas mixtures in the linear range i.e. 0–0.517 kg/h in percentage format so that it could be an accurate error evaluation index for the total mass flow rate as well.

According to the figure, although the error profiles of all of the mixtures fluctuate along the mass flow rate axis, the maximum error values of all of the gases are observed in mass flow rate equal to 0.086 kg/s and the highest error value is 1.8% for Torkman field. Thereafter, the error values of each gas come up and down irregularly. The average error values in the linear range for Pars, Khangiran, Torkman, Bidboland, Gonbadly and Kangan are equal to 0.47%, 0.48%, 0.61%, 0.65%, 0.75% and 0.78%, respectively. The overall average error of all of the gases is 0.62% which is a very satisfactory result.

By far, taking into account the results of simulation and validation presented, one could easily find out that the designed capillary tube thermal flow meter with the characteristics detailed in Table 1 is not affected by changing natural gas compositions and the device could be reliably used for mass flow metering of an arbitrary natural gas mixture in residential consumption flow rate range.

In the final step, the details of selecting the considered characteristics for the sensor tube are discussed. Naturally, after proving this fact that similar results are obtained for all of the considered natural gas fields for a specific sensor tube, one could discuss this matter for only one of these gas fields. Torkman mixture has been chosen for this objective here. In this respect, Fig. 11a–c evaluate respectively the effect of alteration of the sensors position on the sensor tube, the sensor tube length variation and the sensor tube internal and external diameters changes on the linearity range and the sensitivity of the device relative to heat capacity rate change of Torkman gas.

According to Fig. 11a, the longer distance of sensors from the middle of the sensor tube, the higher sensitivities for the capillary tube thermal flow meter are expected, however, the linearity range on the performance graph decreases as the position distance increases. Therefore, one should tradeoff for finding the most appropriate sensor position, taking the degree of importance of linearity range and sensitivity into account. Finally, L_s=7.5 was considered as the suitable distance from the middle of the sensor tube as linearity range up to at least 3×10^{-4} kJ/(K s) is very important in the simulation process. In Fig. 11b, it is well shown that the sensor tube length variation in the considered range affects neither the linearity range nor the sensitivity of the device for Torkman gas. As a result, a sensor tube with the length of 90 mm is chosen for the simulation. In the end, Fig. 11c proves that increasing the sensor tube diameter affects the linearity range considerably. In D_{in}=0.977 mm the profile is totally linear for flow rates up to almost 3×10^{-4} kJ/(K s) while this range decreases down to 2.5×10^{-4} kJ/(K s) and 2×10^{-4} kJ/(K s) for internal diameters of 0.562 mm and 0.364 mm, respectively. It should be

Please cite this article as: S. Parvizi, et al., Natural gas compositions variation effect on capillary tube thermal mass flow meter performance, Flow Measurement and Instrumentation (2016), http://dx.doi.org/10.1016/j.flowmeasinst.2016.07.007

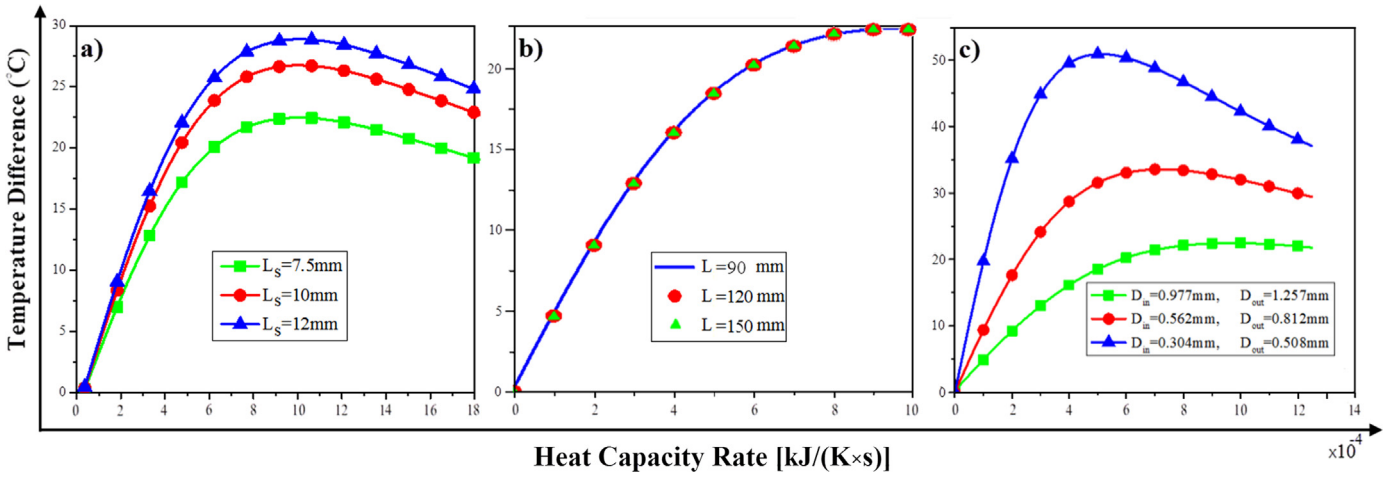

Fig. 11. The effect of changing the sensor tube diameter/length and the sensors positions on the device sensitivity and linearity range for Torkman gas.

mentioned that these three internal diameters were chosen based on the internal diameters and thickness of the sensor tubes available in the market and literature.

5. Conclusion

As there is a significant difference between the amount of natural gas metered in supporting transmission pipeline and the measured value in residential use sector every year, there should be an accurate flow metering device to be replaced instead of the currently in use diaphragm volume flow meters. Employing capillary tube thermal flow meters for this objective has already been proposed, however, the previous study considered natural gas as pure methane. This work investigates the effect of changing natural gas compositions on the device performance and measurement accuracy by considering the actual compositions of 6 main natural gas fields of Iran covering the widest range of heaviness from very light to very heavy gases. The results of simulation show that mass flow rates up to 0.517 kg/s could be measured accurately by the sensor tube of the device provided that it is calibrated based on an accurate operation performance curve. Therefore, having a capillary tube thermal flow meter with 8 tubes the same as its sensor tube in bypass section; one could meter natural gas mass flow rates up to the maximum possible flow rates in residential sector (0–4.5 kg/h). The trend of temperature difference variation measured by the two main sensors on the sensor tube versus specific heat rate changes associated with a mixture with specific heat capacity and density of respectively 2.088 kJ/(kg K) and 0.723 kg/m^3 was finally found as the most accurate operation performance curve. In this way, a maximum error of 1.8% and an overall average error of 0.62% in mass flow metering of all of the considered natural gas mixtures were observed which prove the high accuracy and reliability of the device for an arbitrary natural gas mixture. Also, the effects of natural gas stream pressure and temperature changes, in their widest possible ranges, on the measurement accuracy were investigated, resulting to insignificant influence on the device performance.

References

[1] M. Farzaneh-Gord, M. Farsiani, A. Khosravi, A. Arabkoohsar, F. Dashti, A novel method for calculating natural gas density based on Joule Thomson coefficient, J. Nat. Gas Sci. Eng. 26 (2015) 1018–1029.
[2] J.W. Smalling, L.D. Braswell, L.C. Lynnworth, Apparatus and methods for measuring fluid flow parameters, US Patent 4,596,133, issued June 24, 1986.
[3] AGA8, Compressibility and super compressibility gas and other hydrocarbon gases, Transmission Measurement Committee Report No. 8, AGA Catalogue No. XQ 1285, Arlington, VA., 1992.
[4] M. Farzaneh-Gord, H.R. Rahbari, Developing novel correlations for calculating natural gas thermodynamic properties, Chem. Process Eng. 32 (4) (2011) 435–452.
[5] Il. Young Han, Dong-Kwon Kim, Sung Jin Kim, Study on the transient characteristics of the sensor tube of a thermal mass flow meter, Int. J. Heat Mass Transf. 48 (13) (2005) 2583–2592.
[6] N.R. Chapman, D.W. Etheridge, A step change in domestic metering technology from leather diaphragms to ultrasonic, Flow Meas. Instrum. 5 (2) (1994) 141–142.
[7] Claudemir Duca Vasconcelos, S.érgio Ricardo Lourenço, Antonio Carlos Gracias, Douglas Alves Cassiano, Network flows modeling applied to the natural gas pipeline in Brazil, J. Nat. Gas Sci. Eng. 14 (2013) 211–224.
[8] ⟨http://www.iraniangas.ir/Portal/Home/⟩.
[9] M. Farzaneh-Gord, S. Parvizi, A. Arabkoohsar, L. Machado, R.N.N. Koury, Potential use of capillary tube thermal mass flow meters to measure residential natural gas consumption, J. Nat. Gas Sci. Eng. 22 (2015) 540–550.
[10] F. Cascetta, F. Rampazzo, G. Rotondo, Calibration results of a new generation capillary type thermal mass flowmeter for natural gas, OIML Bull. LIV (4) (2013) 5–11.
[11] Ali Sukru Cubukcu, Diego F. Reyes Romero, Gerald A. Urban, A dynamic thermal flow sensor for simultaneous measurement of thermal conductivity and flow velocity of gases, Sens. Actuators A: Phys. 208 (2014) 73–87.
[12] P. Cappa, Z. Del Prete, F. Marinozzi, Experimental analysis of a new strain-gage signal conditioner based on a constant current method, Sens. Actuators A: Phys. 55 (2–3) (1996) 173–178.
[13] F. Cascetta, A. Piccato, F. Rampazzo, G. Rotondo, G. Spazzini, Metrological characterization of a capillary type thermal mass flowmeter (CTTMF) for natural gas metering, in: Proceedings of FLOMEKO 2013, 16th International Flow Measurement Conference, Paris, 24–26 september 2013, (Conference paper).
[14] ASME MFC-21.2-2010, Measurement of Gas Flow by Means of Thermal Dispersion Mass Flow meters, American Society of Mechanical Engineers, 3 Park Avenue, New York, NY 10016.
[15] J.G. Olin, Industrial Thermal mass flow meters—part 1: principles of operation, Meas. Control 193 (1999) 83–90.
[16] F. Cascetta, G. Rotondo, A. Piccato, P.G. Spazzini, Calibration procedures and uncertainty analysis for a thermal mass gas flowmeter of a new generation, Measurement 89 (2016) 280–287.
[17] K. Komiya, F. Higuchi, K. Ohtani, Characteristics of a thermal gas flow meter, Rev. Sci. Instr. 59 (3) (1988) 477–479.
[18] W. Graebel, Advanced Fluid Mechanics, 2007, ISBN: 978-0-12-370885-4.
[19] A. Arabkoohsar, L. Machado, M. Farzaneh-Gord, R.N.N. Koury, The first and second law analysis of a grid connected photovoltaic plant equipped with a compressed air energy storage unit, Energy 87 (2015) 520–539.
[20] S.J. Kim, S.P. Jang, Experimental and numerical analysis of heat transfer phenomena in a sensor tube of a mass flow controller, Int. J. Heat Mass Transf. 44 (9) (2001) 1711–1724.

Please cite this article as: S. Parvizi, et al., Natural gas compositions variation effect on capillary tube thermal mass flow meter performance, Flow Measurement and Instrumentation (2016), http://dx.doi.org/10.1016/j.flowmeasinst.2016.07.007